Applied Physics Letters ARTICLE scitation.org/journal/apl

Imaging collective behavior in an rf-SQUID metamaterial tuned by DC and RF magnetic fields

Cite as: Appl. Phys. Lett. **114**, 082601 (2019); doi: 10.1063/1.5064658
Submitted: 6 October 2018 · Accepted: 7 February 2019 ·
Published Online: 26 February 2019

Alexander P. Zhuravel,[1] Seokjin Bae,[2] Alexander V. Lukashenko,[3] Alexander S. Averkin,[4] Alexey V. Ustinov,[3,4] and Steven M. Anlage[2,a)]

AFFILIATIONS

[1]B. Verkin Institute for Low Temperature Physics and Engineering, Kharkov 61103, Ukraine
[2]Center for Nanophysics and Advanced Materials, Department of Physics, University of Maryland, College Park, Maryland 20742, USA
[3]Physikalisches Institut, Karlsruhe Institute of Technology, 76131 Karlsruhe, Germany
[4]Russian Quantum Center, National University of Science and Technology MISIS, Moscow 119049, Russia

[a)]**Author to whom correspondence should be addressed:** anlage@umd.edu

ABSTRACT

We examine the collective behavior of two-dimensional nonlinear superconducting metamaterials using a non-contact spatially resolved imaging technique. The metamaterial is made up of sub-wavelength nonlinear microwave oscillators in a strongly coupled 27×27 planar array of radio-frequency Superconducting QUantum Interference Devices (rf-SQUIDs). By using low-temperature laser scanning microscopy, we image microwave currents in the driven SQUIDs while in non-radiating dark modes and identify the clustering and uniformity of like-oscillating meta-atoms. We follow the rearrangement of coherent patterns due to meta-atom resonant frequency tuning as a function of external dc and rf magnetic flux bias. We find that the rf current distribution across the SQUID array at zero dc flux and small rf flux reveals a low degree of coherence. By contrast, the spatial coherence improves dramatically upon increasing the rf flux amplitude, in agreement with simulation.

Planar arrays of deep sub-wavelength dimension superconducting (SC) resonators have recently gained increasing attention due to their potential use as nonlinear metamaterials, i.e., engineered media whose electromagnetic response can differ dramatically from natural materials. Arrays of coupled SC resonators can be used for controllable routing and manipulating electromagnetic wave propagation in the range from radio-frequency (rf)[1,2] through the THz[3,4] domain. Demonstrated effects include electromagnetically[5] and self-induced broadband transparency,[6] negative magnetic permeability,[7] polarization rotation,[8] Fano resonance,[9] and multi-stable states.[10] Extensive progress on the development and applications of SC metamaterials has been achieved.[2,11–20] It has been shown that such SC structures have significant advantages over their normal-metal counterparts allowing reduced losses by several orders of magnitude, shrinking the size of artificial meta-atoms, and achieving tunable frequency of operation by means of macroscopic quantum phenomena.[16,20]

Traditional SC metamaterials are composed of compact, self-resonating spirals and split-ring resonators (SRRs) of different designs.[1,15,16,18,21] Potentially, these structures could be used for switching,[5,10,22] and tuning, by virtue of the dynamic range of controllable manipulation of their resonances with external stimuli.[23,24]

There has been great interest in using radio-frequency Superconducting QUantum Interference Devices: rf-SQUIDs as meta-atoms.[2,7,11,12,16,19,20,22,25,26] Contrary to the SRR and SC spiral, the rf-SQUID incorporates an extremely tunable nonlinear inductor, arising from the Josephson effect, when a Josephson junction (JJ) is incorporated into a SC loop. The loop geometry adds the macroscopic quantum property of flux quantization, which in turn allows one to conveniently control the Josephson inductance through the magnetic flux applied to the loop.[27] The benefits of the rf-SQUID system were originally presented theoretically in the context of an artificial atom with discrete energy levels[12] and extremely strong nonlinearity.[25,28] This system can exhibit negative and/or oscillating effective magnetic permeability which can be wide-band tuned together with the resonance.

Recent experiments on rf-SQUID-based meta-atoms have lived up to most if not all of the theoretical expectations.[17,20] It

has been shown that the rf-SQUID meta-atoms have a rich nonlinear behavior arising from the nonlinearity of the Josephson junction.[10,29] In the case of small rf drive, the tuning capability of the single rf-SQUID is an $n\Phi_0$-periodic function (n is an integer) of the flux quantum $\Phi_0 = h/2e$, while dc magnetic flux (Φ_{dc}) dependent variations of the resonant frequency can reach up to 80 THz/Gauss.[27,30,31] Furthermore, the rf-SQUID demonstrates undistorted, high-Q resonances under tuning by Φ_{dc}.[27,30–32] However, degradation of dc flux tunability and hysteresis behavior has been documented at increased temperature T and rf flux amplitude Φ_{rf}.[6,10,27]

Since the advantages of classical rf-SQUID-based metamaterials are defined by a collective response of oscillating meta-atoms, their natural and/or forced frequency (and phase) synchronization accompanied by coherent tunability are of paramount importance. As with any nonlinear discrete structure, there is a competition between self-organization and destruction of the collective resonant behavior due to disorder[33] and nonlinearity. The degree of spatial-temporal coherence (i.e., frequency and phase synchronization of the meta-atoms)[34] of rf-SQUID metamaterials was previously examined experimentally and theoretically in terms of the collective globally averaged transmission properties.[35] However, many magneto-inductive modes of the metamaterial exist that have very weak coupling to a uniform microwave excitation.[36] Examination of these dark modes[33] and their nonlinear evolution requires a microscopic form of investigation.

The phenomenon of incoherence in large populations of interacting SQUIDs is the subject of intense theoretical and numerical research,[8,27,35,37–40] and in particular, there are clear predictions for the development of Chimera states in rf-SQUID arrays[20,41] (see Refs. 19 and 42 for a review). Here, we present images of the microscopic states and site-dependent coherence of nonlinear and disordered arrays of strongly coupled rf-SQUIDs. We address several important questions: (1) Can coherence be induced by large-amplitude rf driving flux? (2) Does the structure of synchronously coupled rf-SQUIDs remain stable under dc flux tuning? (3) How is this structure spatially modified in the presence of disorder (e.g., due to randomly distributed imperfections during fabrication) and dc flux gradient?

The investigated SC metamaterial consists of 27×27 rf-SQUID meta-atoms equidistantly arranged in a square array with a lattice constant of 83 μm as shown in Figs. 1 and S1 (supplementary material). These rf-SQUIDs are formed on a Si substrate using trilayer Nb/AlO$_x$/Nb Josephson junction (JJ) technology. More details on array fabrication, microwave design, global experimental characterization, and rf simulation of similar rf-SQUID arrays have been described in Refs. 27, 29, 36, and 43 and the supplementary material.

The spatially resolved technique of laser scanning microscopy (LSM) has been employed in the past to image rf current densities and local sources of nonlinearity through a controlled thermal perturbation of superconducting microwave circuits. Thermal perturbation of a dc nano-SQUID has been used before to image local dissipation,[44] and a preliminary study of rf-SQUID LSM has been published.[45] A simplified schematic of this setup is shown in Fig. 1. The rf-SQUID array is placed on a cooled quartz rod between the walls of a specially designed rectangular

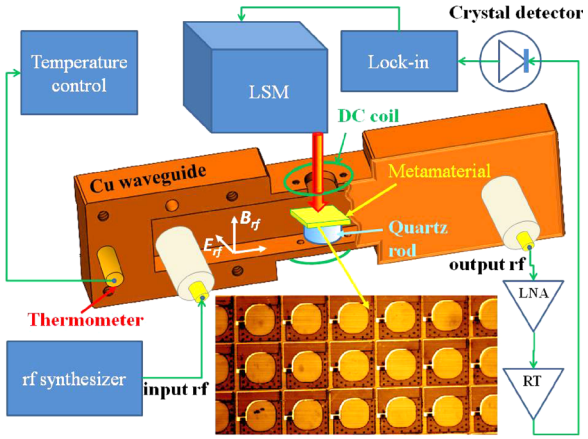

FIG. 1. Schematic representation of the LSM setup used for 2D visualization of microwave photo-response of the rf-SQUID metamaterial. LNA is the low-noise cryogenic amplifier, while RT is a room temperature rf amplifier. The red line denotes the scanned laser beam, while the green circles show the dc magnetic flux coils. Drawing is not to scale. The inset illustrates the LSM optical reflectivity image in a 500×250 μm^2 area of the array.

copper waveguide which has $14 \times 7 \times 80$ mm^3 interior dimensions (single propagating mode from 10.6 to 20 GHz). The rod fixes the array in a region of homogenous rf magnetic field in a way that the magnetic vector of the traveling TE$_{10}$ mode is predominantly perpendicular to the x-y plane of the SQUIDs. Note that the waveguide to coaxial cable transitions are impedance matched, and the single propagating mode provides the rf flux bias to the array. A circular opening in the waveguide wall provides LSM access to the rf-SQUIDs for 2D laser probing of their microwave properties, as well as visible-light reflectivity imaging, which allows for proper alignment of photo-response (PR) images. Two superconducting Helmholtz coils are glued to the waveguide to introduce a homogenous dc magnetic flux orthogonally threading the loops of the rf-SQUIDs. The entire construction is surrounded by mu-metal shielding to shield the rf-SQUIDs from environmental magnetic and electromagnetic influences. Additionally, its temperature is stabilized at $T_0 = 4.5$ K in a specialized optical cryostat with an accuracy of 1 mK, excluding any thermal drift of resonance frequency.

In this work, the rf-SQUIDs are stimulated by a low input rf power $P_{IN} = -60$ dBm, corresponding to rf flux amplitude $\Phi_{rf} \approx 10^{-4}\Phi_0$.[36] The sample is directly illuminated with a laser beam (wavelength 640 nm and laser power $P_L = 10$ μW) that is focused into a 20 μm diameter spot, which is smaller than a single rf-SQUID but larger than a Josephson junction. Its intensity is reduced within the LSM optics down to 3.2×10^2 W/m^2 and modulated at a frequency of $f_M \sim 1$ MHz while the absorbed radiation produces a periodic heating $\delta T < 1$ mK underneath the laser probe (see supplementary material). This laser-beam-induced perturbation is low enough not to change significantly the spatial distribution of resonating currents in the array. The probe scans point-by-point in a raster pattern over the examined area of the array. The maximum area of the LSM raster is 5×5 mm^2 while the minimum step size between its discrete points is 1 μm.

Under these conditions, the dominant effect of the laser beam perturbation is a change of the temperature dependent tunneling critical current I_c of the probed JJ, resulting in the (oscillating at f_M) modification of its Josephson inductance $L_{JJ}(T,\Phi_{app}) = \frac{\Phi_0}{2\pi I_c \cos\delta}$, where δ is the gauge-invariant phase difference on the junction and $\Phi_{app} = \Phi_{dc} + \Phi_{rf}\sin(2\pi f t)$. This causes, in turn, a periodic modulation of the resonant frequency f_0 of the rf-SQUID

$$f_0(T,\Phi_{app}) = \frac{1}{2\pi\sqrt{\left(\frac{1}{L_{geo}} + \frac{1}{L_{JJ}(T,\Phi_{app})}\right)^{-1} C}}, \quad (1)$$

which also oscillates under laser modulated heating. Here, L_{geo} is the geometric inductance of the rf-SQUID loop and C is the shunt capacitance of the JJ such that $f_{geo} = 1/2\pi\sqrt{L_{geo}C}$ is the geometric resonance of the SQUID loop in the absence of a Josephson effect, assuming that the electrodynamics of the SQUID is described by the resistively and capacitively shunted junction (RCSJ) model.[46]

The laser beam induced differences between perturbed and unperturbed resonances cause a modulation of transmitted rf power $PR(\Phi_{app},f) \sim \delta P_{OUT}(\Phi_{app},f) \sim \delta||S_{21}(\Phi_{app},f)||^2$, where $S_{21}(f)$ is the spectral response of the forward transmission coefficient through the waveguide at frequency f. This signal is the LSM photo-response (PR) that is amplified by 67 dB, converted with a crystal diode to voltage $\delta V(t)$ signal and, after demodulation by a phase sensitive lock-in (SR844) technique, is used to create local voltage contrast of the images presented below.

In the regime of weak linear perturbation ($\Phi_{rf} \ll \Phi_0$; $\delta T \ll T_c$), and excluding nonlocal and nonequilibrium effects (see Ref. 47 and references therein), the resonant spectrum of the LSM $PR(\Phi_{app}, f)$ can be modeled[48–51] through additive contributions from two different origins. The first contribution is due to the shift of the resonant frequency profile $f_0(T, \Phi_{app})$ under laser illumination. As depicted in Fig. 3 of Ref. 27, a local temperature rise in a SQUID under illumination decreases the critical current I_c, resulting in a shift of f_0 at a fixed Φ_{dc}. This PR component due to the f_0 shift is called inductive PR[49]

$$PR_X \propto P_{IN}\frac{\partial|S_{21}(\Phi_{app},f)|^2}{\partial f}\delta f_0, \quad (2)$$

where P_{IN} is the input rf power, and PR_X can be positive or negative, depending on Φ_{app} and f.

The second origin for PR is due to the change in quality factor Q. As the local temperature rises under the laser illumination, the dissipation increases from the quasiparticle current flowing via the tunneling resistance R_N of the JJ, decreasing the Q of the $|S_{21}|$ resonance dip, resulting in resistive PR,[49] which has a uniform sign as a function of frequency or flux[49]

$$PR_R \propto P_{IN}\frac{\partial|S_{21}(\Phi_{app},f)|^2}{\partial(1/2Q)}\delta(1/2Q). \quad (3)$$

Thus, the evolution of photoresponse with frequency or dc flux helps to reveal its origins. Note that both PR_X and PR_R are proportional to the local rf current squared under the laser illumination, at least in the linear response regime.[48–50] (see Sec. S9 of the supplementary material) As a result, the photoresponse is dramatically reduced outside the resonant spectrum of the rf-SQUID.

With the LSM, we first have the opportunity to probe the *global* tuning properties of the rf-SQUID metamaterial through a measurement of the *local* PR from a single SQUID in the middle of the array as the globally applied Φ_{dc}/Φ_0 is varied over several periods. The resulting $PR(\Phi_{dc}, f)$ from the JJ in a SQUID near the center (12-th row, 14-th column) of the array over the range of $f = 10.6$ GHz (cutoff frequency of the waveguide) to 20 GHz (the maximum measurement frequency of the LSM electronics) is shown in Fig. 2. A clear tunability of the resonant response of the meta-atom with dc flux is evident, consistent with earlier results obtained through global transmission measurements of the entire metamaterial.[6,7,27,31] The periodic tunability of the resonant response (bright areas in Fig. 2) vs. magnetic flux is clearly visible with maximum value at $\Phi_{dc} = n\Phi_0$, while a minimum of f_0 is achieved at $\Phi_{dc} = (n+1/2)\Phi_0$, where n is an integer. The strong PR features are reasonably well described by a simulated curve[27,36] for $f_0(T, \Phi_{app})$ from Eq. (1), shown by the orange line, assuming that L_{JJ} varies through all values of $\cos\delta$ as a function of flux.

Additionally, despite observing a similar degree of tuning capability in all of the locally probed rf-SQUIDs in the array, we measured that their individual resonances are widely distributed over the full flux range. In other words, there is a significant spread of natural resonances when a small rf driving flux ($10^{-4}\Phi_0$ in this case) is applied to the rf-SQUIDs (see supplementary material S5).

We now address the smeared out LSM PR of a single rf-SQUID in the array close to zero dc flux as shown between 17 and 20 GHz in Fig. 2. This PR is distinctly different from that of a single isolated SQUID (Fig. S5 of the supplementary material). Figure 3(a) presents the experimental $\Phi_{dc} = 0$ cut of PR from Fig. 2. On the basis of the global transmission measurement,[6,7,27,31]

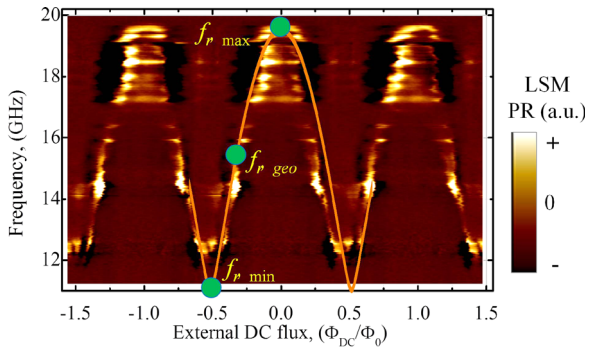

FIG. 2. Measured LSM photo-response of an individually probed rf-SQUID near the middle (12-th row, 14-th column) of a 27 × 27 rf-SQUID metamaterial as a function of frequency and reduced external dc flux Φ_{dc}/Φ_0 at −60 dBm rf power ($\Phi_{rf} \approx 10^{-4}\Phi_0$) and 4.8 K. The resonant response is outlined by the brightest areas in a false color presentation. The orange solid line containing green circles of reference frequencies is calculated from Eq. (1).[27,36]

one would naively expect PR($\Phi_{dc} = 0, f$) to exist only at one frequency, namely, $f = f_0(T, \Phi_{dc} = 0)$. However, this profile of LSM PR($\Phi_{dc} = 0, f$) displays a spectrum of resonances in the wide range of 18.5–20 GHz, which is the range of expected magneto-inductive modes of the metamaterial.[36,39] We find that the shape of this profile is scarcely modified with variation of dc flux up to $0.2\Phi_0$ and thus we limit the spatially resolved LSM PR investigation only to the frequency domain. Two-dimensional LSM imaging of the resonant pattern formation was done by scanning the entire area of the array by the same laser spot that was used for the local probing. A typical scanned frame consists of 600×600 points of PR. Only resonating rf-SQUIDs are visible, with the PR being dominated by bright spots at the locations of the associated JJs.

In Fig. 3(b), we present LSM photo-response observed at the isolated PR resonance near 18.9 GHz [see Fig. 3(a)]. At an input rf power of $P_{IN} = -60$ dBm ($\Phi_{rf} \approx 10^{-4}\Phi_0$), roughly half of the rf-SQUIDs show large-amplitude PR spatially grouping together in the left part of the array, with virtually no PR on the right side of array. As seen in Figs. 3(c)–3(e), starting from $f = 19.45$ GHz and up to 19.9 GHz, the distribution of excited SQUIDs is spatially varying as a function of driving frequency. Their structure forms stationary patterns of large clusters showing response of the rf-SQUIDs having nearly degenerate resonances. Also, LSM images in Figs. 3(b), 3(d), and 3(e) contain dissipative response (PR_R) from limited numbers of defective JJs (details are given in supplementary material Sec. S8). The diagonal movement of the PR structure from the upper right to the lower left corner of the array with the increase in rf frequency [Figs. 3(c)–3(e)] implies a gradient in either rf-SQUID properties or perhaps in the dc flux applied to the metamaterial.[27,36] A similar experimentally observed (but not illustrated) diagonal redistribution of the LSM PR under varied global DC flux can also be noted, and such an effect is described below.

A pattern with strong spatial coherence involving a majority of the rf-SQUIDs is formed by applying a stronger rf driving field at $P_{IN} = -40$ dBm ($\Phi_{rf} \approx 10^{-3}\Phi_0$) as shown in Fig. 3(f). One can see a dome-like distribution of strongly responding rf-SQUIDs which is expected to occur in systems of coherent rf-SQUIDs in the lowest-order magneto-inductive eigenmode of the array.[35,36,39] Such a transition was observed in simulations of a 21×21 array as the driving amplitude activated the nonlinearity.[36]

The next question to examine is the influence of small variations of external dc magnetic flux on the spatial stability of the coherent state. For this purpose, we apply an external dc flux $\Phi_{dc} = 0.35\Phi_0$ to obtain at an arbitrarily chosen frequency $f_0 = 14.4$ GHz $< f_{geo}$ a coherent pattern under $P_{IN} = -45$ dBm ($\Phi_{rf} \approx 5.6 \times 10^{-4}\Phi_0$) with the same distribution of LSM PR as shown in Fig. 3(f). Additional DC flux increases with equal steps $\Delta\Phi_{dc} = 0.02\Phi_0$ to explore the spatial evolution of this pattern under magnetic detuning in a flux regime showing strong tunability. The upper row of LSM PR images in Fig. 4 shows resonant patterns of the rf-SQUID oscillators starting from $\Phi_{dc} = 0.35\Phi_0 + 0.02\Phi_0$ while the bottom row presents the LSM images for conjugated Φ_{dc} with an increase by 2 or 3 flux quanta.

The observed coherent states are clearly different from the dome-like structure in Fig. 3(f). The distributions in Figs. 4(a)–4(c) demonstrate progressive excitation of the SQUIDs near the geometric edges of the array. The SQUIDs near the edges of the array witness a different combined dc + rf flux because they have fewer nearest neighbors than those in the center of the array.[35,36] As the dc flux is tuned, the edge SQUIDs come into resonance, at the expense of those in the middle of the array.

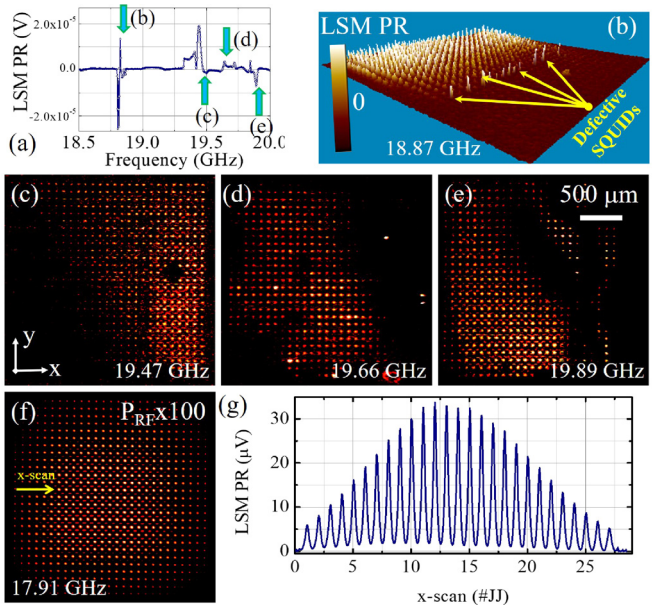

FIG. 3. (a) Frequency dependence of the LSM PR of an individually probed rf-SQUID located near the center of the array, at zero dc flux, −60 dBm rf power ($\Phi_{rf} \approx 10^{-4}\Phi_0$), and 4.8 K. (b) 3D and (c)–(f) 2D LSM PR maps showing the shape and position of resonant clusters at different frequencies of (b) 18.87 GHz, (c) 19.47 GHz, (d) 19.66 GHz, and (e) 19.89 GHz. (f) Pattern of PR at 17.91 GHz produced by 100 times increased rf power, $P_{in} = -40$ dBm ($\Phi_{rf} \approx 10^{-3}\Phi_0$). (g) An x-line cut of PR through the center line of the array [yellow line in (f)].

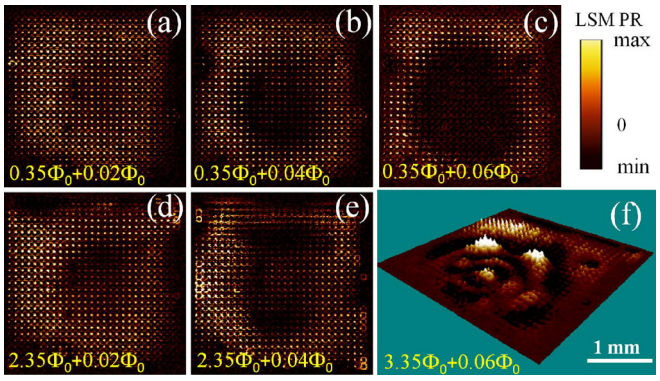

FIG. 4. DC magnetic flux dependent clustering of the spatially coherent pattern in the 27×27 rf-SQUID array that is generated by small steps of extra applied dc flux (starting from $\Phi_{dc} = 0.35\Phi_0$) of (a) $0.02\Phi_0$, (b) $0.04\Phi_0$, and (c) $0.06\Phi_0$. Modification of the coherent structure by integer flux quanta of (d) and (e) $2\Phi_0$ and (f) $3\Phi_0$. The image in (f) is presented in 3D to clearly show the development of clusters. Here, $P_{rf} = -45$ dBm ($\Phi_{rf} \approx 5.6 \times 10^{-4}\Phi_0$) and $f = 14.4$ GHz are fixed through (a)–(f).

The naïve expectation is that $n\Phi_0$ flux quantization in the array will lead to repetition of the same spatial pattern at any n of additional DC flux bias. Figures 4(d) and 4(e) demonstrate that this is true to some extent. However, small distortions and the development of a number of additional clusters are evident compared to the structure shown in Figs. 4(a) and 4(b). A frequency splitting of the rf-SQUID metamaterial *global* response was noted earlier at Φ_0 and $2\Phi_0$.[35] Hence, we believe that these spatial features arise from two effects: (1) increase in the DC flux gradient[35,36] and (2) spatial modification of resonating currents caused by defective SQUIDs.

In summary, we have visualized the microscopic dark-mode states of a large nonlinear metamaterial structure using the LSM technique. The spatial variation of rf-SQUID excitation can now be elucidated while tuning driving frequency as well as dc and rf flux amplitudes. Our experiments show that the degree of coherence of the SQUID excitations is strongly enhanced for larger rf flux amplitude and is diminished by defects and inhomogeneous DC flux.

See supplementary material for the referenced discussion. The raw data are available in Ref. 52.

This work was supported by Volkswagen Foundation Grant No. 90284, DFG Grant No. US18/15, MESRF Contract No. K2-2017-081, NSF Grant No. DMR-1410712 (S. Bae in Karlsruhe), and DOE Grant Nos. DESC0017931 (S. Bae in Maryland) and DESC0018788 (S. M. Anlage).

REFERENCES

[1]C. Kurter, J. Abrahams, and S. M. Anlage, Appl. Phys. Lett. **96**, 253504 (2010).
[2]S. M. Anlage, J. Opt. **13**, 024001 (2011).
[3]N. I. Zheludev and Y. S. Kivshar, Nat. Mater. **11**, 917 (2012).
[4]G. Scalari, C. Maissen, S. Cibella, R. Leoni, and J. Faist, Appl. Phys. Lett. **105**, 261104 (2014).
[5]C. Kurter, P. Tassin, A. P. Zhuravel, L. Zhang, T. Koschny, A. V. Ustinov, C. M. Soukoulis, and S. M. Anlage, Appl. Phys. Lett. **100**, 121906 (2012).
[6]D. Zhang, M. Trepanier, O. Mukhanov, and S. M. Anlage, Phys. Rev. X **5**, 041045 (2015).
[7]S. Butz, P. Jung, L. V. Filippenko, V. P. Koshelets, and A. V. Ustinov, Opt. Express **21**, 22540 (2013).
[8]J.-G. Caputo, I. Gabitov, and A. I. Maimistov, Phys. Rev. B **91**, 115430 (2015).
[9]B. Luk'yanchuk, N. I. Zheludev, S. A. Maier, N. J. Halas, P. Nordlander, H. Giessen, and C. T. Chong, Nat. Mater. **9**, 707 (2010).
[10]P. Jung, S. Butz, M. Marthaler, M. V. Fistul, J. Leppäkangas, V. P. Koshelets, and A. V. Ustinov, Nat. Commun. **5**, 3730 (2014).
[11]M. Ricci, N. Orloff, and S. M. Anlage, Appl. Phys. Lett. **87**, 034102 (2005).
[12]C. Du, H. Chen, and S. Li, Phys. Rev. B **74**, 113105 (2006).
[13]A. L. Rakhmanov, A. M. Zagoskin, S. Savel'ev, and F. Nori, Phys. Rev. B **77**, 144507 (2008).
[14]C. Kurter, A. P. Zhuravel, J. Abrahams, C. L. Bennett, A. V. Ustinov, and S. M. Anlage, IEEE Trans. Appl. Supercond. **21**, 709 (2011).
[15]V. Savinov, V. A. Fedotov, S. M. Anlage, P. A. J. De Groot, and N. I. Zheludev, Phys. Rev. Lett. **109**, 243904 (2012).
[16]P. Jung, A. V. Ustinov, and S. M. Anlage, Supercond. Sci. Technol. **27**, 073001 (2014).
[17]A. V. Ustinov, IEEE Trans. Terahertz Sci. Technol. **5**, 22 (2015).
[18]A. S. Averkin, A. Karpov, A. P. Zhuravel, L. V. Filippenko, V. P. Koshelets, S. M. Anlage, and A. V. Ustinov, IEEE Trans. Appl. Supercond. **27**, 1502204 (2017).
[19]N. Lazarides and G. P. Tsironis, Phys. Rev. E **98**, 012207 (2018).
[20]N. Lazarides and G. Tsironis, Phys. Rep. **752**, 1 (2018).
[21]N. Maleeva, A. Averkin, N. N. Abramov, M. V. Fistul, A. Karpov, A. P. Zhuravel, and A. V. Ustinov, J. Appl. Phys. **118**, 033902 (2015).
[22]N. I. Zheludev, Science **328**, 582 (2010).
[23]M. C. Ricci, H. Xu, R. Prozorov, A. P. Zhuravel, A. V. Ustinov, and S. M. Anlage, IEEE Trans. Appl. Supercond. **17**, 918 (2007).
[24]M. Lapine, I. V. Shadrivov, and Y. S. Kivshar, Rev. Mod. Phys. **86**, 1093 (2014).
[25]N. Lazarides and G. P. Tsironis, Appl. Phys. Lett. **90**, 163501 (2007).
[26]A. I. Maimistov and I. R. Gabitov, Opt. Commun. **283**, 1633 (2010).
[27]M. Trepanier, D. Zhang, O. Mukhanov, and S. M. Anlage, Phys. Rev. X **3**, 041029 (2013).
[28]J.-G. Caputo, I. Gabitov, and A. I. Maimistov, Phys. Rev. B **85**, 205446 (2012).
[29]D. Zhang, M. Trepanier, T. Antonsen, E. Ott, and S. M. Anlage, Phys. Rev. B **94**, 174507 (2016).
[30]P. Jung, S. Butz, S. V. Shitov, and A. V. Ustinov, Appl. Phys. Lett. **102**, 062601 (2013).
[31]S. Butz, P. Jung, L. V. Filippenko, V. P. Koshelets, and A. V. Ustinov, Supercond. Sci. Technol. **26**, 094003 (2013).
[32]A. Vidiborskiy, V. P. Koshelets, L. V. Filippenko, S. V. Shitov, and A. V. Ustinov, Appl. Phys. Lett. **103**, 162602 (2013).
[33]S. D. Jenkins, N. Papasimakis, S. Savo, N. I. Zheludev, and J. Ruostekoski, Phys. Rev. B **98**, 245136 (2018).
[34]N. Papasimakis, V. A. Fedotov, Y. H. Fu, D. P. Tsai, and N. I. Zheludev, Phys. Rev. B **80**, 041102 (2009).
[35]M. Trepanier, D. Zhang, O. Mukhanov, V. P. Koshelets, P. Jung, S. Butz, E. Ott, T. M. Antonsen, A. V. Ustinov, and S. M. Anlage, Phys. Rev. E **95**, 050201 (2017).
[36]M. Trepanier, Ph.D. thesis (University of Maryland, 2015), http://drum.lib.umd.edu/handle/1903/17290.
[37]A. B. Cawthorne, P. Barbara, S. V. Shitov, C. J. Lobb, K. Wiesenfeld, and A. Zangwill, Phys. Rev. B **60**, 7575 (1999).
[38]J. A. Acebrón, L. L. Bonilla, C. J. Pérez Vicente, F. Ritort, and R. Spigler, Rev. Mod. Phys. **77**, 137 (2005).
[39]N. Lazarides and G. P. Tsironis, Supercond. Sci. Technol. **26**, 084006 (2013).
[40]N. Lazarides, G. Neofotistos, and G. P. Tsironis, Phys. Rev. B **91**, 054303 (2015).
[41]J. Hizanidis, N. Lazarides, and G. P. Tsironis, Phys. Rev. E **94**, 032219 (2016).
[42]M. J. Panaggio and D. M. Abrams, Nonlinearity **28**, R67 (2015).
[43]D. Yohannes, A. Kirichenko, S. Sarwana, and S. K. Tolpygo, IEEE Trans. Appl. Supercond. **17**, 181 (2007).
[44]D. Halbertal, J. Cuppens, M. B. Shalom, L. Embon, N. Shadmi, Y. Anahory, H. R. Naren, J. Sarkar, A. Uri, Y. Ronen, Y. Myasoedov, L. S. Levitov, E. Joselevich, A. K. Geim, and E. Zeldov, Nature **539**, 407 (2016).
[45]A. S. Averkin, A. P. Zhuravel, P. Jung, N. Maleeva, V. P. Koshelets, L. V. Filippenko, A. Karpov, and A. V. Ustinov, IEEE Trans. Appl. Supercond. **26**, 1800403 (2016).
[46]K. K. Likharev, *Dynamics of Josephson Junctions and Circuits* (Gordon and Breach, Philadelphia, 1986).
[47]R. Gross and D. Koelle, Rep. Prog. Phys. **57**, 651 (1994).
[48]A. P. Zhuravel, A. G. Sivakov, O. G. Turutanov, A. N. Omelyanchouk, S. M. Anlage, A. Lukashenko, A. V. Ustinov, and D. Abraimov, Low Temp. Phys. **32**, 592 (2006).
[49]A. P. Zhuravel, S. M. Anlage, and A. V. Ustinov, Appl. Phys. Lett. **88**, 212503 (2006).
[50]A. P. Zhuravel, S. M. Anlage, and A. V. Ustinov, IEEE Trans. Appl. Supercond. **17**, 902 (2007).
[51]A. P. Zhuravel, S. Bae, S. N. Shevchenko, A. N. Omelyanchouk, A. V. Lukashenko, A. V. Ustinov, and S. M. Anlage, Phys. Rev. B **97**, 054504 (2018).
[52]A. P. Zhuravel, S. Bae, and S. M. Anlage, see http://hdl.handle.net/1903/21732.